Large-area metamaterials on thin membranes for multilayer and curved applications at terahertz and higher frequencies

X. G. Peralta,[1,a] M. C. Wanke,[1] C. L. Arrington,[1] J. D. Williams,[1] I. Brener,[1] A. Strikwerda,[2] R. D. Averitt,[2] W. J. Padilla,[3] E. Smirnova,[4] A. J. Taylor,[4] and J. F. O'Hara[4]
[1]*Sandia National Laboratories, Albuquerque, New Mexico 87185, USA*
[2]*Department of Physics, Boston University, Boston, Massachusetts 02215, USA*
[3]*Department of Physics, Boston College, Chestnut Hill, Massachusetts 02467, USA*
[4]*Los Alamos National Laboratory, Los Alamos, New Mexico 87545, USA*

(Received 12 November 2008; accepted 13 March 2009; published online 24 April 2009)

A possible path for fabricating three-dimensional metamaterials with curved geometries at optical and infrared frequencies is to stack flexible metamaterial layers. We have fabricated highly uniform metamaterials at terahertz frequencies on large-area, low-stress, free-standing 1 μm thick silicon nitride membranes. Their response remains comparable to that of similar structures on thick substrates as measured by the quality factor of the resonances. Transmission measurements with a Fourier transform infrared spectrometer highlight the advantage of fabricating high frequency metamaterials on thin membranes as etalon effects are eliminated. Releasing the membranes enables layering schemes and placement onto curved surfaces in order to create three-dimensional structures. © *2009 American Institute of Physics*. [DOI: 10.1063/1.3114416]

For the past few years, metamaterials have attracted considerable attention partly due to the promise of devices that exploit their electromagnetic properties, which are not readily available in naturally occurring materials.[1–3] While much effort has been devoted to one-dimensional structures based on planar arrays of metallic metamaterial units on a dielectric substrate, two- and three-dimensional (3D) structures still remain challenging to fabricate at terahertz (THz), infrared, and visible frequencies, although they are required for many of the proposed applications.[2,4] Some of these challenges arise from fabrication approaches based on rigid (quartz, Si, GaAs) substrates with high dielectric constants that are thick ($\sim$600–1000 μm) compared with the target wavelength. Other approaches have centered on stacking single layers (tens of microns thick)[5–7] or multilayer processing[8,9] but have been limited to planar implementations and small areas (<1 cm^2). In an effort to address these issues, we have developed a process to fabricate metamaterials on large-area, free-standing, thin silicon nitride (Si_3N_4) membranes. Membrane based metamaterials can be formed into 3D structures by folding,[10] layering, removing them from the host substrate, placing them onto curved surfaces, or a combination of the above. Unlike the only other report of metamaterials fabricated on 100 nm silicon nitride membranes,[11] our membranes are 1 μm, thick enough to allow some manipulation but thin enough to be ductile and conform to various curved surfaces. Moreover, fabricating metamaterials on thin membranes offers other advantages: it lowers the effective permittivity of the supporting media, an important feature for sensing applications,[12] and it reduces the dielectric losses due to the substrate and enables simple transmission measurements at higher frequencies than in comparable thick substrate based metamaterials where etalon effects can confound the results.

We chose to fabricate metamaterials with a resonant response in the terahertz range (f=0.1–10 THz, λ=3000–30 μm) due to ease of fabrication and the availability of powerful broadband phase sensitive measurement techniques [time-domain spectroscopy (TDS)]. In addition, the scalability of the designs allows us to use the terahertz range as a test bed for different designs that can be scaled to other frequencies of interest.[13,14] Single-layer metamaterials were fabricated on 4 in., 550 μm thick Si wafers coated with 1 μm, low-stress Si_3N_4 using plasma enhanced chemical vapor deposition (PECVD). In order to open windows to the metamaterials on the front side at a later processing step, four Si_3N_4-free windows were defined on the back side of the wafer using reactive ion etching. The front side of the wafer was patterned with 15 different metamaterial designs using evaporated Ti/Au (200 Å/500 Å) and lift-off techniques. The wafer was subsequently mounted in a wafer holder, which protects the front side in order to remove the Si substrate from the Si_3N_4-free windows by immersing it in a KOH bath. For more details on the fabrication procedure, see Ref. 15. When removed from the wafer holder, the metamaterials are patterned onto four, free-standing, $\sim$(3.0 $\times$ 2.3) cm^2, 1 μm Si_3N_4 windows (see center inset of Fig. 1). All windows are divided into quadrants, each with a different metamaterial design covering a $\sim$(1.4$\times$1) cm^2 area. Visual inspection reveals highly uniform patterning across that area. One quadrant in one of the windows was intentionally left unpatterned to use as a reference.

In order to understand the effect of having a thin Si_3N_4 membrane as a substrate for terahertz metamaterials (membrane thickness$\leqslant$300 μm$\sim$1 THz), we measured the transmission properties (phase and amplitude) of all 15 metamaterial designs. We used a terahertz TDS system based on photoconductive antennas for both the source and the detector at room temperature in a dry ($<$1% relative humidity) air atmosphere.[16] The polarization of the optical field was perpendicular to the gaps and transmitted normal to the plane of the metamaterials [see insets of Figs. 1(a) and 1(c)]. The time-varying electric fields of the terahertz transmitted light through the unpatterned Si_3N_4 membrane and through

[a]Electronic mail: xomalin.peralta@utsa.edu.

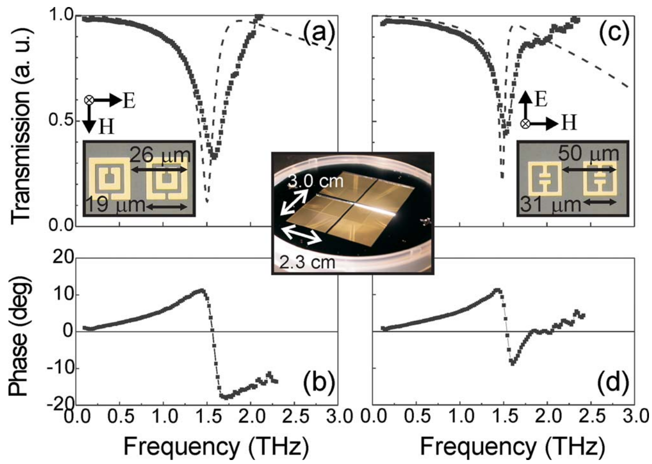

FIG. 1. (Color online) Transmission spectra (solid dots) and simulation results (dashed line) for (a) double SRR (dSRR) and (c) electrical resonator (E2). [(b) and (d)] Corresponding phase data. Center inset: fully processed wafer where the Si_3N_4 membrane windows are evident.

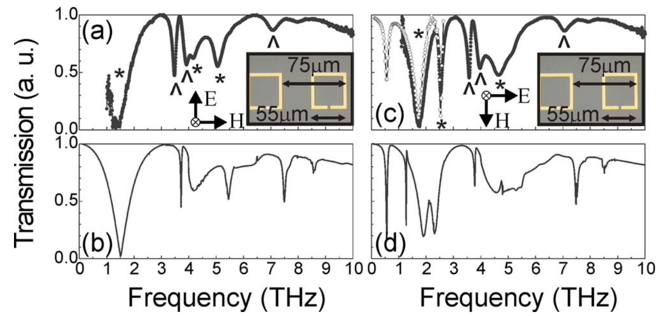

FIG. 2. (Color online) Comparison of [(a) and (c)] experimental transmission spectra and [(b) and (d)] simulation results for the SRR. Terahertz electric field polarized [(a) and (b)] parallel and [(c) and (d)] perpendicular to the gap. In (c) open (solid) circles correspond to THz-TDS (FTIR) measurements.

each of the metamaterial designs were recorded. The normalized terahertz transmission electric field amplitude spectra for each design were obtained by performing a numerical Fourier transform of the corresponding time-varying electric field and dividing it by the reference spectrum. The phase data were obtained by taking the phase difference between the sample and the reference. Figure 1 shows representative data for two different metamaterials designed to operate at 1.5 THz. Both metamaterials present a spectrally selective resonant decrease in transmission [Figs. 1(a) and 1(c)], while the phase data show the dispersive line shape characteristic of Lorentzian resonances [Figs. 1(b) and 1(d)]. The dashed lines in Figs. 1(a) and 1(c) show the results of finite-element modeling using CST MICROWAVE STUDIO.[17] The modeling results also indicate that the observed resonances are the result of induced circulating currents associated with inductor-capacitor (LC) resonances.

Having a 1 μm thick Si_3N_4 membrane as a substrate shifts the Fabry–Pérot oscillations due to reflections outside of our region of interest; therefore we were able to extend the characterization spectral range (1–10 THz) using a Fourier transform infrared (FTIR) spectrometer equipped with terahertz optics. Measurements were performed at room temperature in vacuum. Unlike the TDS technique, the FTIR measurement is incoherent; therefore it only provides the normalized transmission electric field amplitude spectra. The results for a metamaterial design consisting of a single splitring resonator (SRR) are presented for terahertz radiation polarized parallel [Fig. 2(a)] and perpendicular [Fig. 2(c)] to the gaps and transmitted at normal incidence (see insets). In both cases we observe multiple resonances, some of which are polarization dependent (asterisk) while others are not (arrows). For terahertz radiation perpendicular to the gap [Fig. 2(c)], we were able to match the positions of the low frequency resonances obtained from both, the TDS (open symbols) and the FTIR (solid) measurements to within, at most 2%. There are more significant differences between the transmission minima values as well as line widths of the resonances, which are still under investigation. We speculate that they may be accounted for by the excitation dynamics of the standing-wave plasmon modes responsible for the resonant response[18] and their interaction with a ~10 ps long pulse compared to a continuous wave, incoherent source.

We also performed electromagnetic modeling using finite-element software and were able to reproduce qualitatively most of the features observed in the measurements and their relative positions for both polarizations as shown in Figs. 2(b) and 2(d). There are several possible explanations for the differences observed. A constant permittivity and loss tangent value for bulk Si_3N_4 at 9.5 GHz were used in the simulations as frequency dependent values for Si_3N_4 membranes were unavailable in the terahertz region. There can also be variations between the ideal, simulated devices and the imperfect, fabricated ones as well as limited resolution in the modeling of thin membranes. The differences observed in the 1–3 THz region might be due to the effect of higher-order modes.[19] Note that at frequencies above 4 THz we are no longer within the effective medium approximation as at that point the periodicity (75 μm) becomes comparable to the wavelength.

In order to compare the performance of the metamaterials on Si_3N_4 membranes with those previously fabricated on thick substrates, we calculated the quality factor $Q=\omega_0/\Delta\omega$ of the LC resonance for some of our designs and similar ones found in the literature, where ω_0 is the resonant frequency and $\Delta\omega$ is the full width at half maximum. The samples chosen from the literature had the same geometrical shape as our designs with either very similar geometrical parameters to ours or very similar resonance positions. From this comparison [see Fig. 3(a)], it is evident that the structures fabricated on Si_3N_4 membranes have comparable, although slightly smaller, Q's to similar structures that appear in the

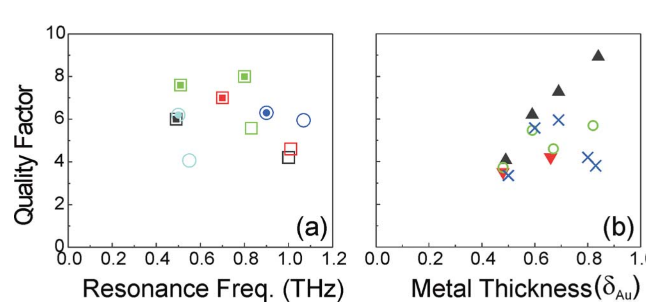

FIG. 3. (Color online) (a) Quality factor extracted from the measured transmission spectra as a function of resonance frequency. Solid (open) symbols were obtained from the literature (metamaterials on Si_3N_4 membranes). Squares (circles) have similar geometry (resonant frequency). (b) Quality factor as a function of metal thickness in units of skin depth for SRR (▲), E1 (▼), E2 (○), and dSRR (×) on Si_3N_4 membranes.

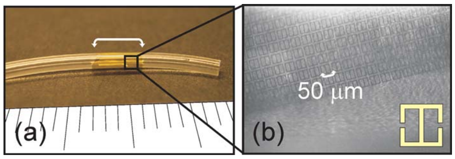

FIG. 4. (Color online) (a) Metamaterial covered membrane wrapped around Tygon tubing. Minor ticks on ruler are millimeters. (b) Zoom in showing the electric metamaterial E1 units.

literature. To understand this result we need to consider the role of the substrate, or lack thereof, and the effect of coupling between resonators due to modified fringing fields as well as the metallization thickness, which is less than the skin depth (δ) of the terahertz radiation, at 1 THz $\delta_{Au} \sim 75$ nm and $\delta_{Ti} \sim 325$ nm. The thickness of Ti used in these samples renders it completely transparent within this frequency range, whereas the thickness of Au is comparable to δ_{Au}. To examine the role of δ_{Au} in determining Q, we plot Q as a function of the Au thickness normalized by δ_{Au} at the resonance position for the 15 metamaterial designs fabricated on Si_3N_4 [Fig. 3(b)]. Keeping in mind that the shape, size, and periodicity of the metamaterials contribute to Q, we note that for the SRR, E1 (see Fig. 4) and E2 designs there is a clear trend toward increasing Q as the Au thickness approaches δ_{Au}. This observation is supported by recent investigations on the role played by the metallization thickness on the resonant features.[20] From the analysis presented in that study, by increasing the metallization thickness we may get up to a 50% decrease in the transmission minima value, which could translate into an increase in Q. A Au thickness of 2500 Å would allow for optimal operation at frequencies of >0.1 THz.

Once the metamaterial covered membrane is fabricated, it can be removed from the Si wafer and placed onto a host material, which can be planar or a curved 3D object. Figures 4(a) and 4(b) show a piece of metamaterial covered membrane, which was removed from the wafer and wrapped around a 1.5 mm diameter Tygon tubing without breaking, highlighting the ductility of the membrane. Proper selection of the material used to support the membrane can ensure that it will not interfere with the metamaterials' electromagnetic behavior, or that it will do so in some desired manner.

We have fabricated highly uniform metamaterials on large-area, low-stress, free-standing, 1 μm thick Si_3N_4 membranes as potential building blocks for 3D metamaterials with curved geometries. Although implemented at terahertz frequencies, this procedure can be extended to optical and infrared frequencies. We characterized their response using THz-TDS and FTIR spectroscopy. From the former we conclude that their low frequency resonant response remains comparable to that of similar metamaterials fabricated on thick, rigid substrates with high dielectric constants. The latter illustrates the advantage, for characterization purposes, of fabricating high frequency metamaterials on thin membranes where etalon effects are eliminated. We also present evidence that the metamaterial covered membrane can be removed from the surrounding wafer and placed onto a curved surface. The present work enables the study of nearly free-standing metamaterials and their fabrication into curved 3D structures at terahertz and higher frequencies.

We acknowledge support from the CINT and the IC Postdoctoral Research Fellowship Program (X.G.P.). Sandia is a multiprogram laboratory operated by Sandia Corporation, a Lockheed Martin Co., for the U.S. DOE's NNSA under Contract No. DE-AC04-94AL85000. Los Alamos National Laboratory, an affirmative action/equal opportunity employer, is operated by Los Alamos National Security, LLC, for the NNSA of the U.S. DOE under Contract No. DE-AC52-06NA25396.

[1] J. B. Pendry, A. J. Holden, D. J. Robbins, and W. J. Steward, IEEE Trans. Microwave Theory Tech. **47**, 2075 (1999).
[2] R. A. Shelby, D. R. Smith, and S. Schultz, Science **292**, 77 (2001).
[3] D. R. Smith, W. J. Padilla, D. C. Vier, S. C. Nemat-Nasser, and S. Schultz, Phys. Rev. Lett. **84**, 4184 (2000).
[4] D. Schurig, J. J. Mock, B. J. Justice, S. A. Cummer, J. B. Pendry, A. F. Starr, and D. R. Smith, Science **314**, 977 (2006).
[5] M. Gokkavas, K. Guven, I. Bulu, K. Aydin, R. S. Penciu, M. Kafesaki, C. M. Soukoulis, and E. Ozbay, Phys. Rev. B **73**, 193103 (2006).
[6] B. D. F. Casse, H. O. Moser, J. W. Lee, M. Bahou, S. Inglis, and L. K. Jian, Appl. Phys. Lett. **90**, 254106 (2007).
[7] A. K. Azad, H.-T. Chen, A. J. Taylor, E. Akhadov, N. R. Weisse-Bernstein, and J. F. O'Hara, arXiv:0804.4880.
[8] N. Katsarakis, G. Konstantinidis, A. Kostopoulos, R. S. Penciu, T. F. Gundogdu, M. Kafesaki, E. N. Economou, Th. Koschny, and C. M. Soukoulis, Opt. Lett. **30**, 1348 (2005).
[9] N. Liu, H. Guo, L. Fu, S. Kaiser, H. Schweizer, and H. Giessen, Nature Mater. **7**, 31 (2008).
[10] P. Stellman, T. Buchner, W. J. Arora, and G. Barbastathis, J. Microelectromech. Syst. **16**, 932 (2007).
[11] M. C. Martin, Z. Hao, A. Liddle, E. H. Anderson, W. J. Padilla, D. Schurig, and D. R. Smith, Conference Proceedings of IEEE IRMMW-THz 2005 (unpublished).
[12] J. F. O'Hara, R. Singh, I. Brener, E. Smirnova, J. Han, A. J. Taylor, and W. Zhang, Opt. Express **16**, 1786 (2008).
[13] C. M. Soukoulis, S. Linden, and M. Wegener, Science **315**, 47 (2007).
[14] W. J. Padilla, D. R. Smith, and D. N. Basov, J. Opt. Soc. Am. B **23**, 404 (2006).
[15] X. G. Peralta, C. L. Arrington, J. D. Williams, A. Strikwerda, R. D. Averitt, W. J. Padilla, J. O'Hara, and I. Brener, Proceedings of MRS Spring Meeting, San Francisco, CA, 24–28 March 2008 (unpublished).
[16] J. F. O'Hara, J. M. O. Zide, A. C. Gossard, A. J. Taylor, and R. D. Averitt, Appl. Phys. Lett. **88**, 251119 (2006).
[17] CST MICROWAVE STUDIO 2008, Computer Simulation Technology, Wellesley Hills, MA, (www.cst.com).
[18] C.-Y. Chen, S.-C. Wu, and T.-J. Yen, Appl. Phys. Lett. **93**, 034110 (2008).
[19] J. F. O'Hara, E. Smirnova, H.-T. Chen, A. J. Taylor, R. D. Averitt, C. Highstrete, M. Lee, and W. J. Padilla, J. Nanoelectron. Optoelectron. **2**, 90 (2007).
[20] R. Singh, E. Smirnova, A. J. Taylor, J. F. O'Hara, and W. Zhang, Opt. Express **16**, 6537 (2008).